Journal of Power Sources 270 (2014) 201–207

Contents lists available at ScienceDirect

Journal of Power Sources

journal homepage: www.elsevier.com/locate/jpowsour

Highly active carbon-supported Pt nanoparticles modified and dealloyed with Co for the oxygen reduction reaction

Bing Li [a, b, *], Zeyu Yan [a, b], Qiangfeng Xiao [c], Jun Dai [a, b], Daijun Yang [a, b], Cunman Zhang [a, b], Mei Cai [c], Jianxin Ma [a, b]

[a] School of Automotive Studies, 4800 Caoan Road, Tongji University, Shanghai 201804, PR China
[b] Clean Energy Automotive Engineering Center, Tongji University, Shanghai 201804, PR China
[c] Research & Development Center, General Motors, Warren, MI 48090, United States

HIGHLIGHTS

- The carbon-supported Pt modified with Co synthesized via an ethylene glycol method.
- Effect of different synthesis conditions investigated.
- PtCo/C demonstrates superior ORR activity and cell performance.
- Dealloying treatment is highly effective for improving catalyst performance.

ARTICLE INFO

Article history:
Received 15 May 2014
Received in revised form
9 July 2014
Accepted 10 July 2014
Available online 22 July 2014

Keywords:
Ethylene glycol (EG)
PtCo/C
Dealloying
Oxygen reduction reaction (ORR)
Proton exchange membrane fuel cell (PEMFC)

ABSTRACT

Highly active carbon-supported Pt modified with transition metal Co catalysts are synthesized by an ethylene glycol (EG) reduction method as cathode electro-catalyst for proton exchange membrane fuel cell (PEMFC) applications. Synthesis conditions, such as precursor, dealloying and heat treatment are investigated to obtain the PtCo/C catalyst with the optimum performance. The active component particles are uniformly dispersed on Vulcan XC-72 support with a narrow particle size distribution centered around 2–4 nm. Energy dispersive X-ray spectroscopy (EDX) results indicate that the catalyst sample contains negligible Co contents with the addition of HCl. Cyclic voltammetry (CV) and linear sweep voltammetry (LSV) reveal that the PtCo/C electro-catalyst with cobalt (II) acetate tetrahydrate as precursor shows better performance than commercial Pt/C, for which electrochemical surface area and oxygen reduction reaction (ORR) performance of mass activity are as high as 54.25 $m^2\ g_{Pt}^{-1}$ and 0.089 A mg_{Pt}^{-1}, respectively. Membrane electrode assemblies (MEAs) prepared with all as-synthesized electro-catalyst samples are tested under different temperatures and relative humidity conditions. The PtCo/C electro-catalyst synthesized with cobalt (II) acetate tetrahydrate as precursor also exhibits highest MEA power density. Herein, the as-synthesized PtCo/C is considered to be promising cathode electro-catalyst to improve the utilization of platinum in PEMFC applications.

1. Introduction

The proton exchange membrane fuel cell (PEMFC) holds a great deal of advantages such as high energy conversion efficiency, quick start-up, low operation temperature and low emission. Therefore, it has been regarded as a potential alternative energy source to conventional fossil-fuel [1]. Governments, enterprises, and research institutions have paid great attention to its development and a wealth of breakthroughs has been made on the structure and key technology of PEMFC. But there are still lots of problems remaining, for instance, reducing the manufacture cost and increasing the activity and durability of the electro-catalyst [2–4]. It is widely recognized that the oxygen reduction reaction (ORR) is an important cathode reaction, which severely restricts the performance of PEMFC due to its slow kinetics [5–7]. Moreover, high loading and well dispersed Pt/C is usually adopted as PEMFC cathode catalyst [8,9], owing to its catalytic activity and stability.

* Corresponding author. School of Automotive Studies, 4800 Caoan Road, Tongji University, Shanghai 201804, PR China. Tel.: +86 21 6958 3891; fax: +86 21 6958 3850.
E-mail address: libing210@tongji.edu.cn (B. Li).

http://dx.doi.org/10.1016/j.jpowsour.2014.07.056
0378-7753/

However, this is also hindering the commercialization for the price and scarcity of Pt. Hence, it is of great significance to develop novel catalyst with superior ORR activity to enhance the cathode performance of PEMFC and effectively lessen the dependence on noble metal Pt. At present, considerable efforts have been devoted to prepare of Pt/C with uniform dispersion and develop Pt-based alloys or catalysts with modified nanostructure in pursuit of these goals [10–14].

Recently, the ethylene glycol (EG) method has been largely used to prepare highly dispersed Pt-based and non-Pt catalyst for its simple operation and scale-up process and great performance improvement [15–18]. Li et al. [13] prepared Pt/C catalyst with different synthesis procedure and found that the catalyst synthesized by EG method displayed both better ORR activity and single cell performance. Yang and coworkers [19,20] conducted a series of studies on carbon supported Ir-based catalysts prepared by modified EG method and prepared Ir–V nanoparticle as PEMFC anode catalyst with a maximum power density of 1008 mW cm^{-2} at 0.6 V and 70 °C, which was 50% higher than that for commercial available Pt/C catalyst [21].

On the other hand, Pt-based alloys with transition metals are helpful to improve the kinetics of the ORR in terms of a more favorable Pt–Pt surface interatomic distance [22,23] or the exposure of more active crystallographic facets [24]. Dealloying treatment, through the selective dissolution of elemental components from an alloy, remains the reduced Pt–Pt distance of alloy and leads to higher surface roughness and more defects [25–28], which may contribute to better electro-catalytic activity. Gan et al. [29] synthesized carbon supported dealloyed Pt_xNi_{1-x} catalysts by potential cycling in N_2-saturated 0.1 M $HClO_4$ and these catalysts showed 4–5 fold enhancements in the mass activity compared with commercial Pt/C. Wang et al. [30] used two methods to dealloy the Cu_3Pt/C intermetallic nanoparticles and revealed that the chemically leached samples (spongy nanoparticles) showed both higher activity and durability for the ORR. Liu et al. [31] synthesized nano-porous Pt–Co alloy nanowires by electrodeposition followed by a dealloying treatment in a mild acidic medium and the product were found to exhibit evidently enhanced methanol oxidation reaction (MOR) activity compared with commercial Pt/C. Excellent performance has also been reported for ORR on Pt-based core–shell catalyst through dealloying treatment [32]. Mani and coworkers [25] made a comparison with electrochemically and chemically dealloying treatment procedure for preparing PtCu core–shell nanoparticle electro-catalysts and found that the electrochemically dealloyed $Pt_{25}Cu_{75}$ displayed the highest Pt mass activity of 0.41 A mg^{-1}_{Pt} in MEA. They also investigated dealloyed ternary $PtNi_3M$ (M = Co, Cu, Fe, Cr) as cathode electro-catalysts, which showed considerable activity improvements in single cell compared to $PtNi_3$ [33]. It is believed that modified d-band structure is weakened for the adsorption energy of reactive intermediates based on the compressive lattice strain of dealloyed Pt, which is responsible for the enhancement in ORR activity [34].

In the present study, the initial carbon supported PtCo nanoparticles were synthesized by a modified EG reducing method. To reveal the advantage of dealloying treatment and obtain the catalyst with superior ORR performance, appropriate amount of HCl solution was added to dissolve the excessive Co near the catalyst surface. Besides, varied reaction conditions as different precursors and heat reduction treatment were studied to determine the optimum synthesis condition. The structure and morphology of the catalysts were characterized using X-ray diffraction (XRD) and transmission electron microscopy (TEM), and the electro-catalytic activities were evaluated through both half-cell and single cell testing.

2. Experimental

2.1. Materials and catalyst synthesis

In a typical synthesis, 0.25 g carbon black (Vulcan XC72, Cabot Corporation) was dispersed in 80 mL EG by mild ultrasonication for 30 min. To obtain the catalyst with Pt loading of 40 wt. % and keep the initial mass ratio of Pt to Co as 10:3, 22.5 mL EG (Sinopharm, Chemical Reagent Co., Ltd.) solution of 0.443 g hexachloroplatinic acid hexahydrate ($H_2PtCl_6 \cdot 6H_2O$, Sinopharm, Chemical Reagent Co., Ltd.) and 0.211 g cobalt (II) acetate tetrahydrate ($C_4H_6CoO_4 \cdot 4H_2O$, Sinopharm, Chemical Reagent Co., Ltd.) or 0.201 g cobalt (II) chloride hexahydrate ($CoCl_2 \cdot 6H_2O$, Sinopharm, Chemical Reagent Co., Ltd.) were added into the above solution and stirred for 2 h, then 5 M NaOH (Sinopharm, Chemical Reagent Co., Ltd.) solution was added into this mixed solution to adjust the pH to 12, and the mixture was refluxed at a temperature of 130 °C for 3 h while still stirring. The catalyst samples synthesized with different precursors are further referred to as PtCo/C ($C_4H_6CoO_4$) and PtCo ($CoCl_2$), respectively. The catalyst without any Co added during the synthesis procedure will be referred as Pt/C. In order to leach the excess Co at catalyst surface, the pH of mixture was finally adjusted to 3 by 2 M HCl (Sinopharm, Chemical Reagent Co., Ltd.) after cooled to room temperature. The catalyst sample synthesized without HCl added will be remarked as PtCo/C (no HCl). The whole reaction process was carried out under nitrogen. The product was collected by filtration and washed several times with ultrapure water, then dried in an oven at 80 °C for 5 h for further use in characterization and electrochemical measurements. In order to study the effect of heat treatment, some catalyst powders were placed in a tube furnace for reduction reaction under a mixture of N_2 and H_2 gas for 2 h with a flow rate of 600 mL min^{-1} for N_2 and 70 mL min^{-1} for H_2, respectively [20]. The catalyst sample synthesized after heat reduction treatment is remarked as PtCo/C (Reduction).

2.2. Physical characterization

The morphology and structure of as-synthesized catalysts were observed using transmission electron microscopy (TEM) analyses, with a JEM 2010 EX microscope, equipped with an energy dispersive X-ray spectrometer (EDX) to determine bulk atomic concentrations, operating at 200 kV. The crystalline phase X-ray diffraction (XRD) patterns were collected on a PHILIPS PW 3040/60 powder diffractometer using CuKα radiation. The working voltage was 40 kV, and the current was 40 mA. The intensity data were collected at 25 °C in a 2θ range of 20°–90° with a scan rate of 1.20° min^{-1}. The microstructural parameters of the samples were determined using JADE6 software [35].

2.3. Electrochemical characterization

For electrochemical evaluation, 2 mg catalyst powder was suspended in 1 mL methanol/Nafion solution (50:1 wt.%) to prepare the catalyst ink. Then, 10 μL of ink was deposited onto a clean glassy carbon (GC) disk electrode (5.6 mm diameter) twice. The overall loading of the mixed catalyst was 0.8×10^{-4} g cm^{-2} for the apparent electrode area of the GC disk (0.247 cm^2). The electrochemical ORR activity of PtCo/C catalyst was tested in a glass cell consisting of a three electrode system in 0.1 M $HClO_4$ electrolyte at 25 °C. A reversible hydrogen electrode (RHE) was used as the reference electrode, and a platinum wire was adopted as the counter electrode. Commercial 40 wt. % Pt/C (Johnson Matthey HiSpec 4000) was also tested for comparison. Cyclic voltammetry (CV) and linear sweep voltammetry (LSV, 1600 rpm) were carried out between 0.05 and 1.15 V vs RHE at a scan rate of 5 mV s^{-1} [36].

2.4. MEA fabrication and single cell performance measurements

The membrane electrode assembly (MEA) was fabricated by the following strategy: (i) The anode ink was prepared by mixing 40 wt. % Pt/C (JM) with a solution of 5% Nafion® ionomer and isopropanol and then sonicated for 4 h. The resulting catalyst ink was directly sprayed onto one side of a membrane (Solvay) at 100 °C to form a catalyst layer giving a metal loading of 0.2 mg_{Pt} cm^{-2}. (ii) For the cathode, the catalyst inks were prepared by mixing as-synthesized catalysts and also 40 wt. % Pt/C (JM) with a solution of 5% Nafion® ionomer and isopropanol. The ratio of catalyst to Nafion® polymer was 3:1. The ink was coated on the other side of the membrane

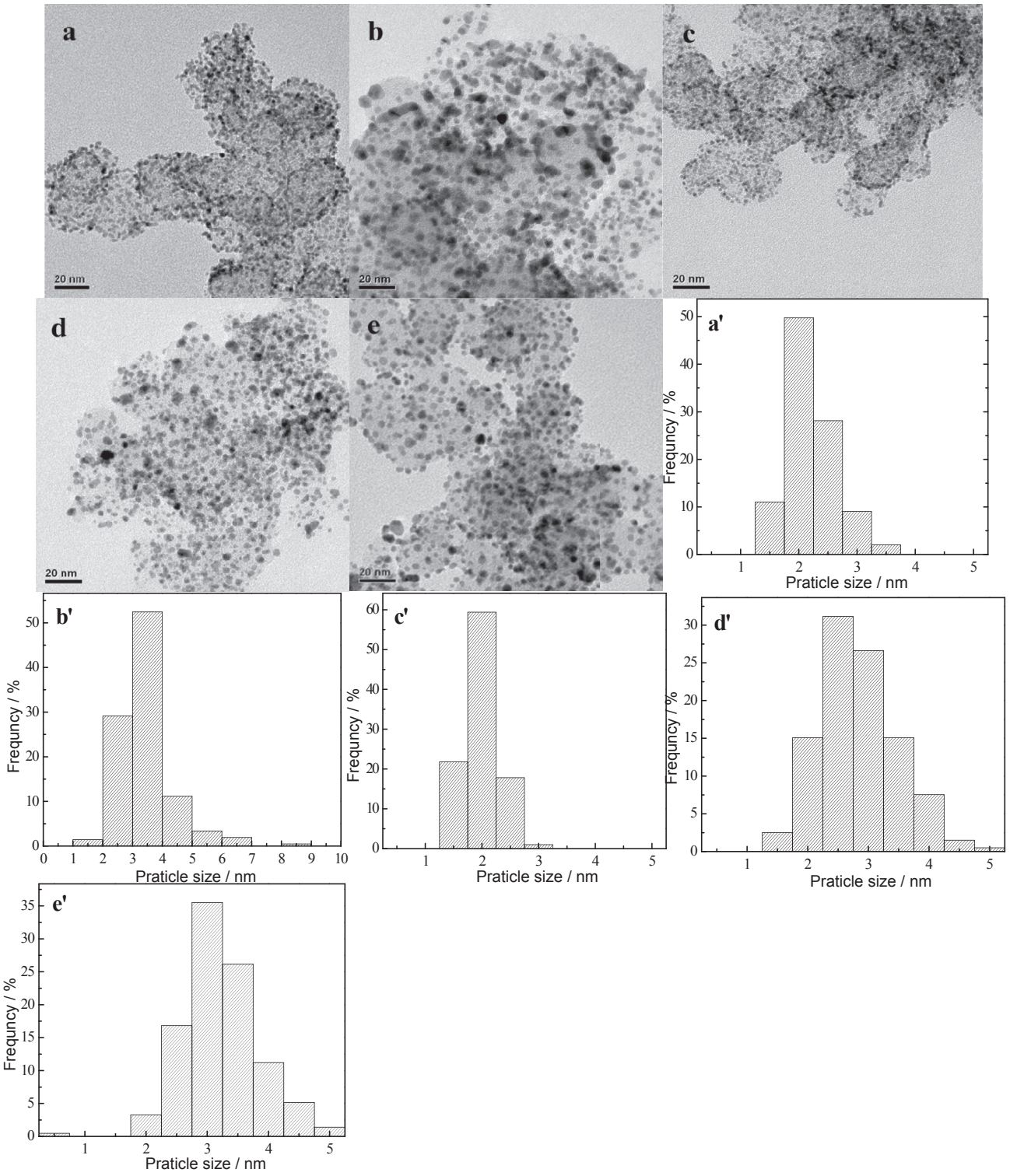

Fig. 1. TEM images of (a) PtCo/C ($C_4H_6CoO_4$); (b) PtCo/C (no HCl); (c) PtCo/C ($CoCl_2$); (d) PtCo/C (reduction) and (e) Pt/C catalysts and particle-size distribution of electro-catalyst samples: (a′) PtCo/C ($C_4H_6CoO_4$); (b′) PtCo/C (no HCl); (c′) PtCo/C ($CoCl_2$); (d′) PtCo/C (reduction) and (e′) Pt/C, respectively.

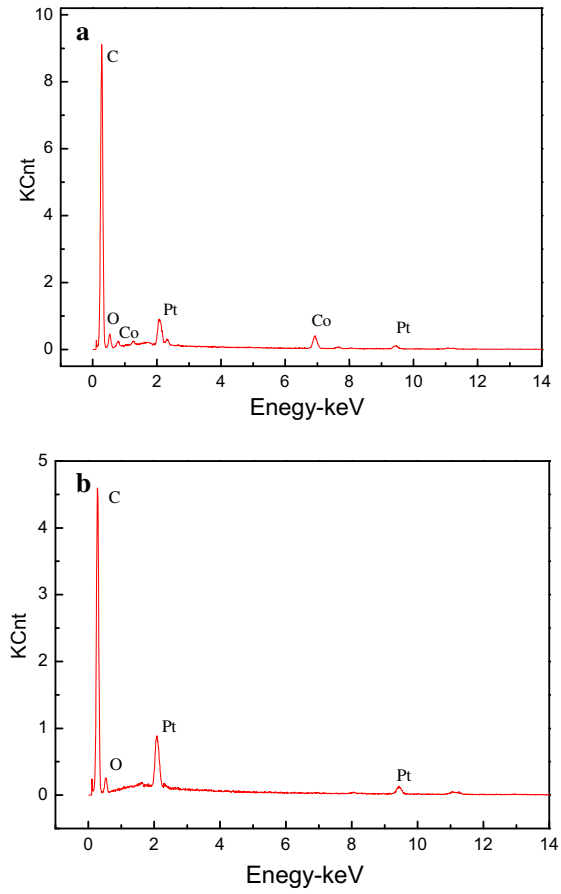

Fig. 2. EDX of (a) PtCo/C (no HCl) and (b) PtCo/C ($C_4H_6CoO_4$) catalysts.

with the same process as the anode, giving a loading of 0.35 mg cm^{-2}. Then two pieces of gas diffusion layers (GDLs) (SGL, 24BC) were just physically placed on each side of the membrane to fabricate the final MEA [37].

The single cell testing was carried out on Green Light (Canada) fuel cell test platform. The flow stoichiometry of H_2 and air were fixed at 1.4 and 2.5, respectively. The temperatures of H_2 and air were maintained at 75 °C by a heating tape and the inlet pressure is 0.1 MPa. To make a comparison about the performance of MEAs with different catalysts, the cell was operated at two groups of different temperatures (73 °C, 90 °C) and relative humidity (50%, 80%), respectively [38].

3. Results and discussion

Fig. 1 presents the TEM images and particle size histograms of all as-synthesized PtCo/C nanoparticle catalysts with different operating processes based on EG reducing method. All samples display small particle size and homogeneous particle dispersion over the

Table 1
Elements content of PtCo/C ($C_4H_6CoO_4$) before and after addition of HCl obtained from EDX.

Element	Wt % (before)	Wt % (after)
Pt	36.54	39.77
Co	5.71	0
C	54.18	54.67
O	3.57	5.56

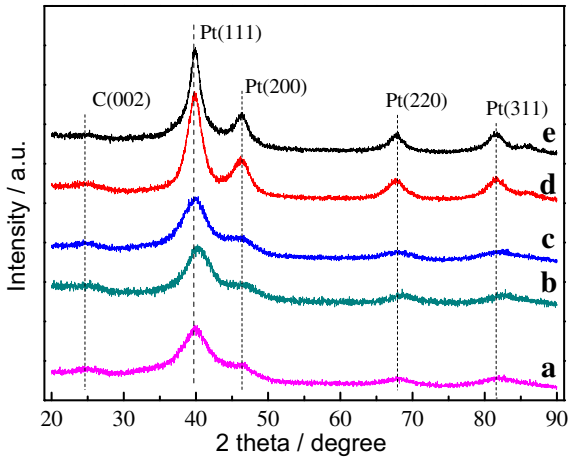

Fig. 3. XRD patterns of as-synthesized catalysts: (a) PtCo/C ($C_4H_6CoO_4$); (b) PtCo/C (no HCl); (c) PtCo/C ($CoCl_2$); (d) PtCo/C (reduction) and (e) Pt/C, respectively.

entire surface area of the carbon support, demonstrating the suitability of the EG method in preparing PtCo/C nanoparticle catalysts. The figure shows apparent luminance difference, indicating that there exists dissimilar element on the carbon support. Pt and Co on the catalyst particles can be clearly identified. Large particles with mean diameter of 3.25 nm are observed for Pt/C (Fig. 1e), which is about 1.34 times than PtCo/C ($C_4H_6CoO_4$), demonstrating that the addition of Co may prevent Pt particles from aggregation, and contribute to smaller catalyst particle sizes. Compared with product prepared with $C_4H_6CoO_4$ (Fig. 1a) as precursor, there's no obvious difference observed on the morphology and particle size of catalyst synthesized with $CoCl_2$ (Fig. 1c) as precursor. The diameters of these two catalysts are 2.27 ($CoCl_2$) and 2.42 ($C_4H_6CoO_4$) nm, respectively. The results suggest that the precursor category has scarce impact on the morphology of the product during EG method preparation. On the contrary, the morphology of as-synthesized catalyst is strongly affected by adding dilute HCl solutions (Fig. 1b). The catalyst prepared without adjusting HCl shows a much bigger diameter of 3.84 nm than other samples. In addition, moderate particle aggregation appears on the catalyst after 200 °C heat reduction treatment for 2 h (Fig. 1d), which contributes to more evident lattice and large particle size. The diameter of this sample increases to 3.06 nm.

EDX spectra (Fig. 2) and Co content (Table 1) were analyzed in order to determine the nanoparticle compositions following the addition of HCl during the EG based deposition. There are no Co peaks observed (Fig. 2b) with the addition of HCl during the deposition which means that the Co on the catalyst surface completely leached away in HCl solutions. Regardless, the presence of Co during particle deposition had a significant impact on the resultant physical and electrochemical properties of the final catalyst materials, and will thus continue to be referred to as PtCo/C.

Table 2
Mean crystallite sizes of as-synthesized PtCo/C electro-catalysts obtained from XRD and TEM.

Catalyst	Lattice parameter (Å)	Mean crystallite size (nm)		
		XRD	TEM	Standard deviation
PtCo/C ($C_4H_6CoO_4$)	3.909	3.1	2.42	0.44
PtCo/C (no HCl)	3.894	4.0	3.84	0.78
PtCo/C ($CoCl_2$)	3.907	2.8	2.27	0.42
PtCo/C (reduction)	3.913	3.7	3.06	0.83
Pt/C	3.913	3.8	3.25	0.71

Table 3
Mass and specific activities for ORR of all electro-catalysts.

Catalyst	Current density at 0.9 V/mA cm^{-2}	Mass activity/ A mg_{Pt}^{-1}	Specific activity/ μA cm_{Pt}^{-2}	Half-wave potential/V
Pt/C (JM)	2.75	0.085	160.7	0.877
PtCo/C ($C_4H_6CoO_4$)	2.89	0.089	164.1	0.881
PtCo/C ($CoCl_2$)	2.55	0.079	198.0	0.876
PtCo/C (no HCl)	1.60	0.049	257.6	0.838
PtCo/C (reduction)	1.59	0.049	120.3	0.849
Pt/C	2.42	0.075	214.4	0.874

Fig. 3 shows the XRD patterns of different as-synthesized PtCo/C electro-catalysts. No diffraction peaks of cobalt are detected in all catalyst samples. The presence of diffraction peaks at 39°, 46°, 67° and 81° could be respectively assigned to Pt (111), Pt (200), Pt (220) and Pt (311), consistent with the face-centered cubic (fcc) structure of Pt. The peak located at 25° can be assigned to the wide graphite (002) peak of the XC-72 carbon black support. Increased diffraction peak intensities are observed for PtCo/C (Reduction) catalyst (Fig. 3d), which indicates better crystallinity of this sample after the heat treatment. Besides, the PtCo/C ($C_4H_6CoO_4$), PtCo/C (no HCl) and PtCo/C ($CoCl_2$) show smaller lattice parameters than the Pt/C sample (Table 2), which suggests that these samples have diminished Pt—Pt distance lattice due to the incorporation of Co atoms. The particle size of Pt was calculated through Debyee Scherrer formula by fitting the full width at half-maximum (FWHM) of the Pt (111) diffraction peak. The diameters of PtCo/C ($C_4H_6CoO_4$), PtCo/C (no HCl), PtCo/C ($CoCl_2$), PtCo/C (Reduction) and Pt/C catalyst particles are about 3.1, 4.0, 2.8, 3.7 and 3.8 nm, respectively (Table 2). The particle sizes have different results by means of TEM and XRD techniques, which may be due to the XRD technology only reflect the crystal grain size, rather than the actual morphology of catalyst [39]. The standard deviation values of particle sizes by means of TEM are also listed in Table 2, which confirms the homogeneous particle dispersion of all samples (Table 3).

The cyclic voltammetry (CV) curves of different as-synthesized PtCo/C and Pt/C (JM) electro-catalysts are shown in Fig. 4. Similar hydrogen adsorption/desorption peaks are observed for as-synthesized PtCo/C electro-catalysts compared with commercial Pt/C (JM). Through the charge transfer for hydrogen adsorption/desorption, the electrochemically active surface areas (ECSA) of Pt/

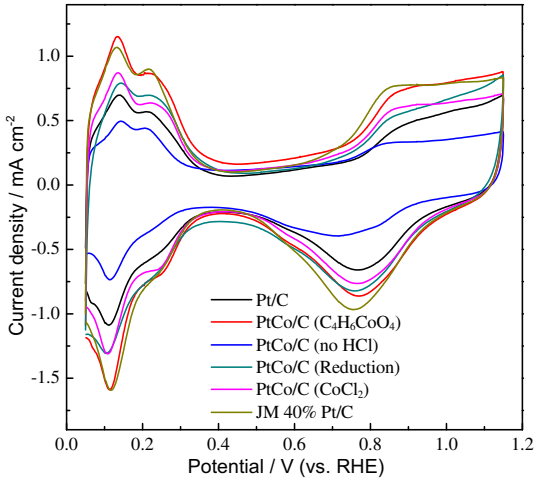

Fig. 4. CV curves of PtCo/C ($C_4H_6CoO_4$); PtCo/C (no HCl); PtCo/C ($CoCl_2$); PtCo/C (reduction); Pt/C and Pt/C (JM) electro-catalysts in N_2-saturated 0.1 M $HClO_4$ at room temperature. Sweep rate: 5 mV s^{-1}.

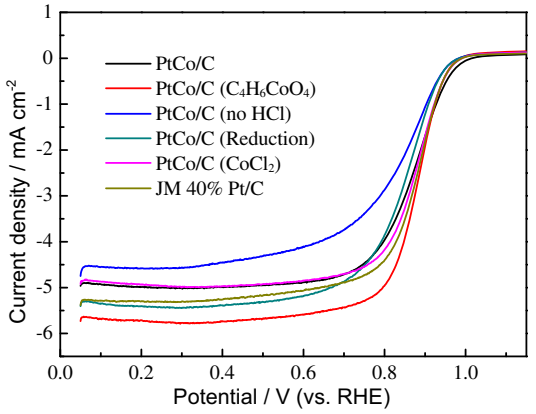

Fig. 5. Linear sweep voltammograms (LSVs) of O_2 reduction on as-synthesized electro-catalysts and commercial Pt/C (JM) in O_2-saturated 0.1 M $HClO_4$ at room temperature. Sweep rate: 5 mV s^{-1}, rotation speed was 1600 rpm.

C (JM), PtCo/C ($C_4H_6CoO_4$), PtCo/C ($CoCl_2$), PtCo/C (no HCl), PtCo/C (Reduction) and Pt/C electro-catalysts are calculated to be 52.90, 54.25, 39.89, 19.02, 40.74 and 34.97 m^2 g_{Pt}^{-1}, respectively. The ECSA of PtCo/C electro-catalysts increase substantially than unmodified Pt/C. The decrease on ECSA of PtCo/C (no HCl) and PtCo/C (Reduction) electro-catalysts can be attributed to their large particle size. Compared with PtCo/C ($C_4H_6CoO_4$) and Pt/C (JM) electro-catalysts, the PtCo/C ($CoCl_2$) shows an evident decline on ECSA although it possesses smallest mean particle diameter. This implies that the

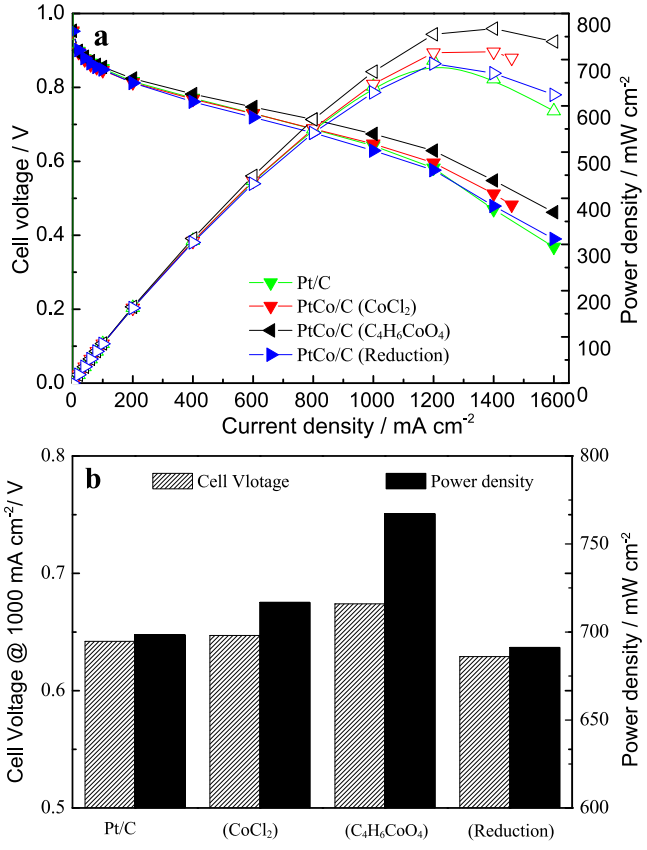

Fig. 6. Performance curves (a) and specific activities (b) of MEA using PtCo/C ($C_4H_6CoO_4$); PtCo/C ($CoCl_2$); PtCo/C (Reduction) and Pt/C as cathode catalysts under 73 °C and RH = 50%.

undersized catalyst particles will not contribute much to the specific activity. It is reported that small Pt nanoparticles are frequently incorporated into the micropores, which always appears to be covered by a thin carbon layer or embedded into the carbon matrix [40]. The ECSA of PtCo/C ($C_4H_6CoO_4$) was slightly higher than that of commercial Pt/C (JM), which indicates the improvement of utilization of Pt by EG method.

In order to characterize the oxygen reduction activity of as-synthesized PtCo/C and Pt/C (JM) electro-catalyst, linear sweep voltammograms are collected and provided in Fig. 5. The onset potentials of all samples are located at about 1.0 V. The mass and specific activities for ORR of all samples are summarized in Table 2. The ORR activity of the series catalysts are in the sequence of PtCo/C ($C_4H_6CoO_4$) > Pt/C (JM) > PtCo/C ($CoCl_2$)/C > Pt/C > PtCo/C (Reduction) > PtCo/C (no HCl). The PtCo/C ($C_4H_6CoO_4$) electro-catalyst shows better ORR performance than Pt/C (JM) with a 4 mV shift of half wave potential towards the positive direction. The PtCo/C ($C_4H_6CoO_4$) and PtCo/C ($CoCl_2$) provided performances superior to that of the unmodified Pt/C, which might be ascribed to the crystal structures modified by Co atoms. Kiros [41] demonstrated a shift to lower lattice parameter of Pt–Co alloy than the pure platinum catalyst, which was considered to be beneficial for more facile oxygen adsorption and oxidation owing to reduced inter-atomic Pt–Pt distance. It can be deduced that the resultant physical and electrochemical properties of the final catalyst materials are significantly affected due to the presence of Co during particle deposition in spite of the fact that the Co on the catalyst surface is thoroughly removed by adding HCl solution. Synthesis procedure with $CoCl_2$ as precursor here is proved to have a negative impact on the ORR activity of the PtCo/C catalyst. Li et al. [13] found that Cl^- brought a negative effect on the ORR performance in both single cell and RDE tests. Because Cl^- can be strongly adsorbed in the active site of Pt surface, thus affecting the oxygen adsorption and reduction, which results in reduced catalyst oxygen reduction activity.

Figs. 6 and 7 show the MEA polarization curves obtained for each as-synthesized electro-catalyst under different relative humidity (RH). For all the catalyst samples, the open-circuit potentials are all almost kept at high level of about 0.95 V. The catalyst samples with higher half-cell performance for the ORR also provide higher MEA maximum power densities in single cell testing, which is generally consistent with the findings in LSV. Interestingly, as compared with Pt/C electro-catalyst, all the PtCo/C samples show enhanced single cell performance under different test conditions. This further confirms the advantages of modification by Co atoms. For example, when tested under T = 73 °C and RH = 50%, the maximum power densities obtained for MEAs fabricated with PtCo/C ($C_4H_6CoO_4$), PtCo/C ($CoCl_2$) and Pt/C are 767.2, 716.8 and 698.4 mW cm^{-2}, respectively. The MEA, which is prepared with PtCo/C ($C_4H_6CoO_4$) as the cathode catalyst, demonstrates the finest performance than other MEAs, generating maximum power densities of 767.2 mW cm^{-2} at RH = 50% and 727.2 mW cm^{-2} at RH = 80%, respectively.

The comparison of single cell performance of PtCo/C ($C_4H_6CoO_4$) and Pt/C (JM) as cathode electro-catalyst is shown in Fig. 8. At given current density of 1000 mA cm^{-2}, the output cell voltage of MEA fabricated with PtCo/C ($C_4H_6CoO_4$) as cathode electro-catalyst reaches 0.674 V (Fig. 8b), which is 0.035 V higher than that of the commercial Pt/C (JM). Besides, the maximum power densities

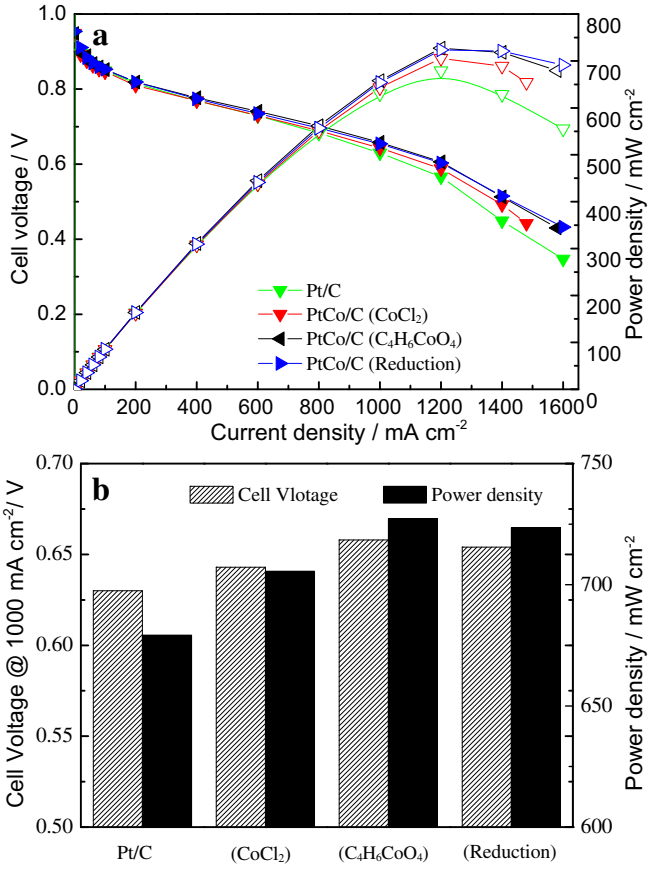

Fig. 7. Performance curves (a) and specific activities (b) of MEA using PtCo/C ($C_4H_6CoO_4$); PtCo/C ($CoCl_2$); PtCo/C (Reduction) and Pt/C as cathode catalysts under T = 73 °C and RH = 80%.

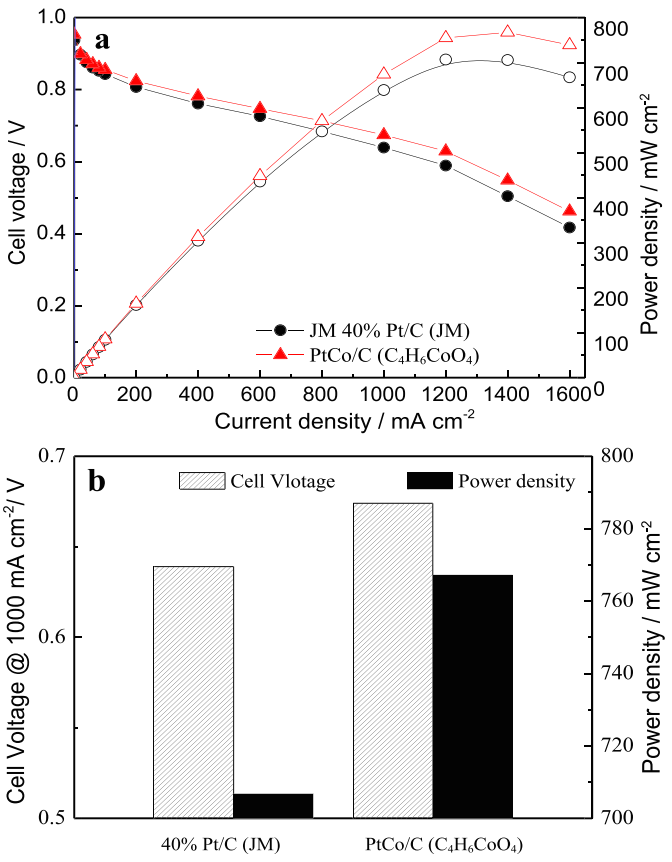

Fig. 8. Performance curves (a) and specific activities (b) of MEA using 40 wt.% Pt/C (JM) and PtCo/C ($C_4H_6CoO_4$) as cathode catalysts under 1 bar, T = 73 °C and RH = 50%.

obtained for PtCo/C ($C_4H_6CoO_4$) and Pt/C (JM) electro-catalyst in the single cell are 767.2 and 706.8 mW cm^{-2}, which also suggests that the PtCo/C ($C_4H_6CoO_4$) shows better MEA performance than commercially available Pt/C. The unique surface structure of carbon supported Pt nanoparticles modified with Co provides more active sites along with diminished Pt–Pt distance, which shows better suitability for oxygen adsorption. Thus, the PtCo/C ($C_4H_6CoO_4$) electro-catalyst displays outstanding ORR activity in both half-cell and single cell testing. Herein, PtCo/C ($C_4H_6CoO_4$) material is presented as a promising replacement to conventional platinum based materials for utilization as cathode electro-catalysts for PEMFC applications.

4. Conclusion

In summary, this study reported the synthesis of active PtCo/C nanoparticle catalyst for PEMFC cathode by applying a modified EG reduction method. The as-prepared PtCo nanoparticles are well dispersed on carbon support and the particles size is mainly distributed at the range of 2–4 nm. The dealloying and heat treatment have tremendous impacted on the morphology of as-prepared PtCo/C catalysts, especially on the particle size which is closely related to the catalytic performance. The optimal synthesis conditions thus determined were employed to prepare PtCo/C nanoparticles catalyst. The as-synthesized PtCo/C ($C_4H_6CoO_4$) catalyst showed better ORR activity than state-of-the-art Pt/C (JM) with a 4 mV shift of half-wave potential towards positive direction. In addition, the MEA fabricated with PtCo/C ($C_4H_6CoO_4$) as cathode catalyst also exhibited higher cell voltage at any given current than other catalysts in the single cell test. With the results presented herein, the novel PtCo/C ($C_4H_6CoO_4$) nanoparticle is strongly suggested to be a promising cathode catalyst for PEMFC.

Acknowledgment

The authors appreciate the National Natural Science Foundation (No. 21206128), International Postdoctoral Exchange Fellowship Program China (201372) and China MoST (2012AA110501) and Henkel Professorship of Tongji University for the financial support of this work.

References

[1] B.L. Yi, Fuel Cells, Chem. Ind. Press, Beijing, 2003.
[2] M. Nie, L.Y. Zhang, Q. Li, B. He, Surf. Technol. 6 (2012) 109–111.
[3] F.F. Liu, M. Lu, Tele. Power Technol. 3 (2009) 25–28.
[4] M. Hou, H.M. Yu, B.L. Yi, Prog. Chem. 11 (2009) 2319–2330.
[5] H.W. Liang, X. Cao, F. Zhou, C.H. Cui, W.J. Zhang, S.H. Yu, Adv. Mater. 23 (2011) 1467–1471.
[6] S.H. Sun, F. Jaouen, J.P. Dodelet, Adv. Mater. 20 (2008) 3900–3904.
[7] S.H. Guo, D.G. Li, H.Y. Zhu, S. Zhang, N.M. Markovic, V.R. Stamenkovic, S.H. Sun, Angew. Chem. Int. Ed. 52 (2013) 3465–3468.
[8] H.F. Xu, Z.Y. Lin, Y.L. Qiu, Q. Tang, Chin. J. Catal. 24 (2003) 143–148.
[9] B. Fan, Y.G. Guo, L.J. Wan, Prog. Chem. 22 (2010) 852–859.
[10] L. Gancs, T. Kobayashi, M.K. Debe, R. Atanasoski, A. Wieckowski, Chem. Mater. 20 (2008) 2444–2454.
[11] A. Bonakdarpour, K. Stevens, G.D. Vernstrom, R. Atanasoski, A.K. Schmoeckel, M.K. Debe, J.R. Dahn, Electrochim. Acta 53 (2007) 688–693.
[12] C.H. Cao, R. Lin, T.T. Zhao, Z. Huang, J.X. Ma, Acta Phys. Chim. Sin. 29 (2013) 95–101.
[13] W.Z. Li, Z.H. Zhou, W.J. Zhou, H.Q. Li, X.S. Zhao, G.X. Wang, G.Q. Sun, Q. Xin, Chin. J. Catal. 6 (2003) 465–470.
[14] L. Dubau, M. Lopez-Haro, L. Castanheira, J. Durst, M. Chatenet, P. Bayle-Guillemaud, L. Guétaz, N. Caqué, E. Rossinot, F. Maillard, Appl. Catal. B: Environ. 142-143 (2013) 801–808.
[15] F. Wu, Y.H. Liu, C. Wu, Chin. J. Process Eng. 12 (2009) 1198–1202.
[16] M. Tsuji, M. Kubokawa, R. Yano, Langmuir 23 (2007) 387–390.
[17] B. Li, D.C. Higgins, D.J. Yang, H. Lv, Z.P. Yu, J.X. Ma, Int. J. Hydrogen Energy 38 (2013) 5813–5822.
[18] L.H. Jiang, Dalian Institute of Chemical Physics, Chinese Academy of Sciences, 2005.
[19] D.J. Yang, B. Li, H. Zhang, J.X. Ma, Int. J. Hydrogen Energy 37 (2012) 2447–2454.
[20] B. Li, J.L. Qiao, D.J. Yang, H. Lv, J.X. Ma, ECS Trans. 25 (2009) 613–618.
[21] B. Li, J.L. Qiao, J.S. Zheng, D.J. Yang, J.X. Ma, Int. J. Hydrogen Energy 34 (2009) 5144–5151.
[22] F.J. Lai, W.N. Su, L.S. Sarma, D.G. Liu, C.A. Hsieh, J.F. Lee, B.J. Hwang, Chem. Eur. J. 16 (2010) 4602–4611.
[23] F.H.B. Lima, M.J. Giz, E.A. Ticianelli, J. Braz. Chem. Soc. 16 (2005) 328–336.
[24] S. Koh, P. Strasser, J. Am. Chem. Soc. 129 (2007) 12624–12625.
[25] P. Mani, R. Srivastava, P. Strasser, J. Phys. Chem. C 112 (2008) 2770–2778.
[26] P. Strasser, S. Koh, T. Anniyev, J. Greeley, K. More, C.F. Yu, Z.C. Liu, S. Kaya, D. Nordlund, H. Ogasawara, F. Michael, T.A. Nilsson, Nat. Chem. 2 (2010) 454–460.
[27] X.Q. Li, Q. Chen, I. McCue, J. Snyder, P. Crozier, J. Erlebacher, K. Sieradzki, Nano. Lett. 14 (2014) 2569–2577.
[28] J. Qi, L. Xin, Z.Y. Zhang, K. Sun, H.Y. He, F. Wang, D. Chadderdon, Y. Qiu, C.Y. Liang, W.Z. Li, Green Chem. 15 (2013) 1133–1137.
[29] L. Gan, M. Heggen, S. Rudi, P. Strasser, Nano. Lett. 12 (2012) 5423–5430.
[30] D.L. Wang, Y.C. Yu, H.L. Xin, R. Hovden, P. Ercius, J.A. Mundy, H. Chen, J.H. Richard, D.A. Muller, F.J. DiSalvo, H.D. Abruña, Nano. Lett. 12 (2012) 5230–5238.
[31] L.F. Liu, E. Pippel, R. Scholz, U. Gösele, Nano. Lett. 9 (2009) 4352–4358.
[32] K.C. Neyerlin, R. Srivastava, C.F. Yu, P. Strasser, J. Power Sources 186 (2009) 261–267.
[33] P. Mani, R. Srivastava, P. Strasser, J. Power Sources 196 (2011) 666–673.
[34] M. Oezaslan, P. Strasser, J. Power Sources 196 (2011) 5240–5249.
[35] X. Zhao, M. Yin, L. Ma, L. Liang, C.P. Liu, J.H. Liao, T.H. Lu, W. Xing, Energy Environ. Sci. 4 (2011) 2736–2753.
[36] B. Li, D.C. Higgins, D.J. Yang, H. Lv, Z.P. Yu, J.X. Ma, Int. J. Hydrogen Energy 37 (2012) 18843–18850.
[37] B. Li, J.L. Qiao, D.J. Yang, R. Lin, H. Lv, H.J. Wang, J.X. Ma, Int. J. Hydrogen Energy 35 (2010) 5528–5538.
[38] B. Li, J.L. Qiao, D.J. Yang, J.S. Zheng, J.X. Ma, J.J. Zhang, H.J. Wang, Electrochim. Acta 54 (2009) 5614–5620.
[39] R. Lin, C.H. Cao, T.T. Zhao, Z. Huang, B. Li, A. Wieckowski, J.X. Ma, J. Power Sources 23 (2013) 190–198.
[40] L. Gan, H.D. Du, B.H. Li, F.Y. Kang, New Carbon Mater. 25 (2010) 53–59.
[41] Y. Kiros, J. Electrochem. Soc. 143 (1996) 2152–2157.